

A Quick Primer on Machine Learning in Wireless Communications

Faris B. Mismar

Abstract

This is our final issue of the quick primer on the use of Python to build a wireless communications prototype. This prototype simulates multiple-input and multiple-output (MIMO) systems for a single orthogonal frequency division multiplexing (OFDM) symbol. Further, it shows several artificial intelligence (AI) and machine learning (ML) use cases and introduces the deepwireless library for code implementation. The intent of this primer is to empower the reader with the means to efficiently create reproducible simulations related to AI and ML in wireless communications on inexpensive computing devices. This primer has sprung from a draft aligned with the syllabus of a graduate course (EESC 7v86)—which we created to be first taught in Fall 2022—and has since evolved to where it stands today.

Index Terms

Python, MIMO, OFDM, deepwireless, supervised learning, artificial intelligence, deep learning, convolution, time series, unsupervised learning, reinforcement learning.

I. INTRODUCTION

The research domain of wireless communications and machine learning has been supplied with an abundance of publications, yielding numerous source codes implementing countless assumptions and configurations. These source codes—especially when proprietary or released under restrictive license agreements—can make the idea of reproducibility extremely challenging.

Because of this, and keeping simplicity in mind, we share this quick primer on machine learning in wireless communications in addition to the source code related to it. We call the essential library that implements this primer “deepwireless.” The objective of this primer and

The author is an adjunct associate professor of electrical and computer engineering at The University of Texas at Dallas (email: fbm090020@utdallas.edu).

TABLE I
ABBREVIATIONS

AI	Artificial Intelligence	IDE	Integrated Development Environment	RF	Radio Frequency
BER	Bit Error Rate	KDE	Kernel Density Estimation	RLC	Radio Link Control
BLER	Block Error Rate	LLM	Large Language Model	RNN	Recurrent Neural Network
BS	Base Station	LMMSE	Linear MMSE	RRC	Radio Resource Control
CDL	Clustered Delay Line	LOS	Line Of Sight	RSRP	Reference Signal Received Power
CNN	Convolutional Neural Network	LSTM	Long Short-Term Memory	SDMA	Space-Division Multiple Access
CRC	Cyclic Redundancy Check	MAC	Medium Access Control	SGD	Stochastic Gradient Descent
CSI	Channel State Information	MDP	Markov Decision Process	SINR	Signal to Interference plus Noise Ratio
CoMP	Coordinated Multi-Point	MIMO	Multiple-Input and Multiple-Output	SISO	Single-Input and Single-Output
DFT	Discrete Fourier Transform	ML	Machine Learning	SM	Spatial Multiplexing
DNN	Deep Neural Network	MMSE	Minimum Mean Square Error	SNR	Signal to Noise Ratio
DQN	Deep Q -Network	NLOS	Non-LOS	SVD	Singular Value Decomposition
FEC	Forward Error Correction	OFDM	Orthogonal Frequency Division Multiplexing	UE	User Equipment
FFT	Fast Fourier Transform	PHY	PHYsical	ZF	Zero-Forcing
GAN	Generative Adversarial Network	RE	Resource Element		

the deepwireless library is to fast-track the reader into the ability to build their simulations efficiently using inexpensive computing environments and open-source tools—especially ones with machine learning (ML) and artificial intelligence (AI) applications. Because the wireless communications system of our choice supports multiple-input and multiple-output (MIMO) systems and orthogonal frequency division multiplexing (OFDM), this source code can be used for the prototyping of AI-based air interfaces (AI-AI) for 4G LTE and 5G air interfaces alike. We hope that AI-AI would empower next-generation wireless networks beyond 5G and thus extend the longevity of these libraries and related source code. The deepwireless library and the related source code are written in Python and are available online. Specifically, the deepwireless library is available on GitHub [1] or can be installed using pip and a well-documented source code implementing all the scenarios shown in this primer using deepwireless is available on GitHub. It is no surprise that we have chosen Python to implement deepwireless as Python has become the quintessential programming language for building AI and ML applications due to its simplicity and abundance of supporting libraries. Moreover, it is free to use.

Also, considering the large number of acronyms and abbreviations in this primer, we build a table that can be referenced. These abbreviations can be found in Table I.

II. PROTOCOL STACK

The wireless protocol stack enables communication between devices in cellular networks, facilitating seamless data transmission over the air. The stack is divided into two planes: the user plane and the control plane. The user plane protocol is responsible for handling the actual user data: the content transmitted between end devices (e.g., voice, video, and Internet traffic).

The control plane is responsible for signaling (e.g., to set up, tear down, manage, and maintain user sessions) in the network.

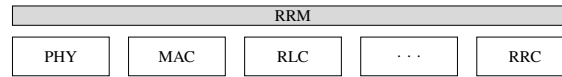


Fig. 1. The control plane air interface protocol stack.

The control plane stack is composed of multiple protocol layers as shown in Fig. 1. We discuss some of them here:

- 1) The physical (PHY) layer: The PHY layer is broken down to two sublayers: low- and high-PHY. The low-PHY sublayer has responsibilities that generally run at a fast time scale and are closer to the radio-frequency (RF) spectrum resources such as time synchronization, frequency alignment, and modulation and coding. The high-PHY sublayer is for functions that operate at slower time scales such as channel equalization, beamforming, and MIMO processing.
- 2) The medium access control (MAC) layer: MAC manages transfers of data in the form of transport blocks, performs retransmission, handles random access contention, and ensures efficient use of the shared radio spectrum. It works closely with the radio link control (RLC) layer, which is responsible for payload segmentation, error detection, retransmissions, flow control, and in-sequence delivery of protocol data units.
- 3) The radio resource control (RRC) layer: This is commonly referred to as “layer-3” signaling. It plays a key role in managing RRC connection management, radio bearers, system information broadcast, paging, area updates, mobility (cell reselections and handovers across base stations, frequency bands, and technologies), and measurement reporting.

Together, the PHY, MAC, and RLC layers enable reliable communication over the air interface by preparing and managing the data transmitted over the network. A key set of procedures that bring together these layers to observe and improve the network performance is radio resource management (RRM). RRM is a group of algorithms for controlling radio parameters to utilize the limited RF spectrum resources and radio network infrastructure as efficiently as possible. Examples of RRM procedures are: power control, precoding, carrier aggregation, interference coordination, link adaptation, scheduling, and mobility management (i.e., handovers and cell reselection).

A valid question is often posed in this context: What *potential* value would AI and ML bring to next-generation wireless network RRM procedures that cannot be realized with “legacy” solutions?

- 1) **Lower latency:** The predictive capability of AI and ML allows the network to prepare an action before it actually happens. This is in contrast with the scenario where the network computes the action reactively (e.g., after a user has moved to the new location as opposed to predicting it).
- 2) **More versatility:** The data-driven approach resulting from UEs reporting their measurements enables model-free systems that can further improve static (and thus highly biased) legacy model-driven models. For example: How often is the noise profile over the air interface truly Gaussian? How does shot noise, especially in large transmission bandwidth, impact the noise profile? In such cases, can symbol detection be done more efficiently for a given channel condition?
- 3) **Better performance:** Legacy and voice-centric RRM procedures such as the configuration of measurement gaps during mobility stem from the days of the third generation wireless standards and still live in 5G NR. These measurement gaps cause data transmission to pause for channel measurements to take place, which in a voice-centric network may not be a perceivable problem. However, with explosive data transmission rates, such measurement gaps can cause a severe degradation in the throughput performance. The use of data-driven intelligence can eliminate these gaps thus improving the performance.
- 4) **More efficient computation:** Several ML algorithms enable parallelization and collaborative learning making use of spare compute power available at neighboring BSs. When an RRM procedure is based on these ML algorithms, it can—unlike legacy RRM procedures—benefit from this advantage for efficiency.

There are also instances where AI and ML should not be applied to wireless network problems. Here are some cases:

- 1) **Costs outweigh benefit:** If training an AI model in a UE can achieve an incremental performance gain at a significant battery life expense, then it should not be done.
- 2) **Problem is well-understood:** If linear calculations can solve the problem, then no need to introduce unnecessary complexity with AI, especially if AI cannot be explained.
- 3) **Data is insufficient:** If UEs do not report often on their pertinent wireless measurements

or if observability is lacking, then collected data could be underestimating ground truth.

- 4) **Real-time requirements:** If the wireless environment changes so rapidly that it becomes impractical to keep invalidating current models and training new ones.
- 5) **Inferior performance:** This is an obvious yet an important one. If introducing AI and ML causes the network performance to degrade, it should not be used.

Now that we sufficiently motivated the protocol stack and the value of introducing AI and ML in wireless networks, we move to the system model next. The system model describes a model-driven implementation, which we contrast with a data-driven implementation. This enables us to then study several RRM procedures formulated as use cases solvable with AI and ML.

III. SYSTEM MODEL

We consider a MIMO* system model with N_t transmit antennas at the base station (BS) with a single OFDM symbol spanning over a number of narrowband subcarriers, the spacing of which is Δf , and N_r receive antennas at the user equipment (UE). The transmitting end has a total power of P_{total} distributed across various transmit antennas such that the signal per antenna has a power of P_x and an energy of E_x . For one OFDM subcarrier, we write the system model as:

$$\mathbf{y} = \mathbf{H}\mathbf{x} + \mathbf{n} \quad (1)$$

where $\mathbf{y} \in \mathbb{C}^{N_r}$ is a column vector containing the received OFDM signal from a transmitted signal column vector $\mathbf{x} \in \mathbb{C}^{N_t}$, which has an average per-antenna power of $\mathbb{E}[\|\mathbf{x}\|^2] := P_x = E_x \Delta f$. Note that $\mathbb{E}[\mathbf{x}\mathbf{x}^*] := \mathbf{R}_{\mathbf{x}\mathbf{x}} = P_x \mathbf{I}_{N_t}$. Thus, $P_{\text{total}} = \text{tr}(\mathbf{R}_{\mathbf{x}\mathbf{x}}) = N_t P_x = N_t E_x \Delta f$. $\mathbf{H} \in \mathbb{C}^{N_r \times N_t}$ is a channel state information (CSI) matrix, and finally $\mathbf{n} \in \mathbb{C}^{N_r}$ is a column vector of additive noise the entries of which are independent and identically sampled from a zero-mean complex Normal distribution $\mathbf{n} \sim \mathcal{N}_{\mathbb{C}}(0, \sigma_n^2)$. The noise power σ_n^2 is further defined with respect to the noise power spectral density N_0 multiplied by the bandwidth of an OFDM subcarrier (i.e., $\sigma_n^2 = N_0 \Delta f$). The number of subcarriers should not exceed the Fast Fourier Transform (FFT) size, which is naturally the smallest power of two that exceeds the number of subcarriers (the difference is given to the guardband subcarriers for robustness against interference). The OFDM symbols are Gray-coded and are either based on M -PSK or M -QAM constellations, with M

*Also applies to the other single-multiple permutations: SISO, MISO, and SIMO systems alike.

being square (i.e., $M \in \{4, 16, 64, 256\}$). We define $k := \log_2 M$ which represents the number of bits transmitted or received per constellation symbol.

The number of streams in this MIMO system N_s is defined as the minimum of the number of antennas in both transmitter and receiver sides. That is, $N_s := \min(N_t, N_r)$. The number of data streams cannot exceed N_s .

The total bandwidth B is computed as the number of subcarriers N_{SC} multiplied by the subcarrier spacing Δf (i.e., $B := N_{\text{SC}}\Delta f$). If we define the capacity with respect to Shannon in bits per second (bps) as $C = B \log_2(1 + \gamma)$, then the spectral efficiency SE (in bps/Hz) is defined as $\text{SE} := C/B$ for a given bit rate C , with γ being the post-equalization signal-to-noise-plus-interference ratio as we define later. Currently, the source code only supports *one user* only; therefore, this model is suitable for a single UE served by a single BS.

Fading: We denote G as the large-scale fading coefficient which can be calculated based on path loss and shadow fading. The calculation of the path loss (PL) depends on several factors such as the desired carrier frequency (f_c), antenna gains on both ends, path loss exponent (η), and distance of the UE from the BS (d). Let us take the example of free space path loss (FSPL), which when excluding the the transmit and receive antenna gains has the formula

$$\text{PL} = \left(\frac{4\pi d}{\lambda} \right)^2 = \left(\frac{4\pi d f_c}{c} \right)^2 \quad (2)$$

from which $\eta = 2$. Also, $\lambda = c/f_c$ is the relationship between the wavelength λ , the carrier frequency, and the speed of light in free space c . As the number of subcarriers become large, applying one large-scale fading value uniformly may no longer be accurate and thus we overload the path loss formula $\text{PL}(f_c)$ to become $\text{PL}(f_i)$ where $f_i = f_c + (i - \frac{N_{\text{SC}}}{2}) \Delta f, i \in \{1, 2, \dots, N_{\text{SC}}\}$.

Besides FSPL, there are other path loss models from industry standards such as the 3GPP urban micro (UMi), urban macro (UMa), and rural macro (RMa). We refer the interested reader to [2] for more details.

For shadow fading, we introduce a Normally distributed random variable with zero mean and unity variance that is multiplied by the shadow fading margin σ_{SF} and then subtracted from the path loss (in dB). Thus, $G_{\text{dB}} := 10 \log(\text{PL}) - \mathcal{N}(0, \sigma_{\text{SF}}^2)$. For a Rayleigh fading channel, the elements of $\mathbf{H} := [h_{ij}]_{i,j}$ are sampled from a zero-mean complex Normal distribution $h_{ij} \sim \mathcal{N}_{\mathbb{C}}(0, 1)$ since the squared modulus of a complex Normal distributed random variable has a Rayleigh distribution. Thus, the power gain of the channel becomes $G \|\mathbf{H}\|_F^2$, which means that

to incorporate the large-scale fading to \mathbf{H} , we simply multiply all the elements of \mathbf{H} by \sqrt{G} . For Ricean fading (with presence of a line-of-sight component between the transmitter and the receiver), the elements of $\mathbf{H} := [h_{ij}]_{i,j}$, $h_{ij} \sim \mathcal{N}_{\mathbb{C}}(\sqrt{\frac{K}{(1+K)}} \frac{1}{K+1})$, where K is the Ricean K -factor (when $K = 0$ we are back to a Rayleigh fading channel).

Alternatively, we introduce the industry standards clustered delay line (CDL) channel models [2] for low complexity simulations since CDLs are statistical representations of the channel that a transmitted signal follows to a receiver for various scenarios: line of sight (LOS), non-line of sight (NLOS), and a combination of both.

Eigenmodes: The channel eigenmodes are the eigenvalues λ_i of $\mathbf{H}\mathbf{H}^*$, each of which is a representation of a parallel spatial data stream enabled by the channel, for what is known as the spatial multiplexing (SM). The value of each eigenmode is the power gain of that stream due to the channel. It is easy to prove that the power gain of the channel is simply the sum of the eigenmodes (i.e., $\|\mathbf{H}\|_F^2 = \sum_{i=1}^{N_r} \lambda_i$). The proof is as follows:

$$\|\mathbf{H}\|_F^2 := \text{tr}(\mathbf{H}\mathbf{H}^*) = \text{tr}(\mathbf{U}\mathbf{\Lambda}\mathbf{U}^{-1}) = \text{tr}(\mathbf{U}^{-1}\mathbf{U}\mathbf{\Lambda}) = \text{tr}(\mathbf{\Lambda}) = \sum_i \lambda_i. \quad (3)$$

In order to exploit these power gains (through means of a precoder \mathbf{F} and the waterfilling algorithm which we briefly describe next), the channel needs to be known at the transmitter. The precoding matrix $\mathbf{F} \in \mathbb{C}^{N_t \times N_s}$ is responsible for both power control and the mapping of the transmit antennas to a number of parallel streams $N_s \leq N_t$.

Precoding and combining: The precoder can be used in order to enable several users to access the same resources at once such as in space-division multiple access (SDMA), cancel interference (i.e., zero-forcing) across different MIMO streams, perform SM, and perform power control per antenna, where the power control matrix can be computed using the waterfilling algorithm (assuming that the channel eigenmodes are known at the transmitter). Waterfilling optimizes the channel capacity by allocating more transmit power towards larger eigenmodes since they have better signal quality. For the transmit diversity mode[†], the Alamouti scheme precoding can be used (MIMO streams are spatially correlated and the same information is sent across multiple antennas to improve robustness). Without precoding, the MIMO system becomes

[†]Beamforming and transmit diversity are two modes in MISO systems. The difference is in the precoding and thus usage: Diversity sends multiple copies of the same signal without having to know the CSI (suitable for areas with low SNR), while beamforming adjusts the transmit phase on these signals to find an optimal signal to interference plus noise ratio (SINR) and thus needs to know the CSI (suitable for high-SNR environments).

a SISO equivalent with the channel gain equal to the largest eigenmode of the channel \mathbf{H} . For the SM mode, where streams are spatially uncorrelated, the capacity of the system is the sum of the capacities of the comprising single channels after decomposing the MIMO channel. Here, the precoder \mathbf{F} and the combiner $\mathbf{G} \in \mathbb{C}^{N_r \times N_r}$ are derived through the singular value decomposition (SVD) of the channel $\mathbf{H} := \mathbf{U}\mathbf{\Sigma}\mathbf{V}^*$ as applied onto the system (1):

$$\begin{aligned}
 \mathbf{y} &= \mathbf{H}\mathbf{x} + \mathbf{n} \\
 &= \mathbf{U}\mathbf{\Sigma}\mathbf{V}^*\mathbf{x} + \mathbf{n} \\
 &= \mathbf{U}\mathbf{\Sigma}\mathbf{V}^* \underbrace{\mathbf{V}\mathbf{s}}_{\mathbf{x}:=\mathbf{F}\mathbf{s}} + \mathbf{n} \\
 &= \mathbf{U}\mathbf{\Sigma}\mathbf{s} + \mathbf{n} \\
 \underbrace{\mathbf{U}^*}_{:=\mathbf{G}}\mathbf{y} &= \mathbf{U}^*\mathbf{U}\mathbf{\Sigma}\mathbf{s} + \mathbf{U}^*\mathbf{n} \\
 \tilde{\mathbf{y}} &= \mathbf{\Sigma}\mathbf{s} + \tilde{\mathbf{n}}
 \end{aligned} \tag{4}$$

where $\mathbf{\Sigma}$ is a diagonal matrix of the square roots of the eigenmodes of the channel \mathbf{H} (or, again, the eigenvalues of $\mathbf{H}\mathbf{H}^*$). It is easy to discern that the precoder $\mathbf{F} := \mathbf{V}$, the combiner $\mathbf{G} := \mathbf{U}^*$, and the diagonalized channel state information is $\mathbf{\Sigma}$. This also implies that the transmitter and the receiver have perfect knowledge of the CSI \mathbf{H} , otherwise the computation of \mathbf{U} and \mathbf{V}^* would not be possible. In words, this system works by applying SVD to the known CSI. Then, the transmitter precodes the transmitted data by pre-multiplying it by \mathbf{V} while the combiner pre-multiplies the signal with \mathbf{U}^* at the receiver end.

Equalization: To get rid of the impact of the channel (or the diagonalized channel for SM), the equalization matrix $\mathbf{W} \in \mathbb{C}^{N_t \times N_r}$ is left-multiplied by the received signal in (1) to obtain

$$\begin{aligned}
 \mathbf{z} &:= \mathbf{W}\mathbf{y} = \mathbf{W}\mathbf{H}\mathbf{x} + \mathbf{W}\mathbf{n} \\
 &= \hat{\mathbf{x}} + \mathbf{v}
 \end{aligned} \tag{5}$$

or, analogously, in (4) to obtain $\mathbf{z} := \mathbf{W}\tilde{\mathbf{y}}$, which is then fed into a symbol detector to identify the originally transmitted OFDM symbols in the presence of the inseparable noise. Equalization also amplifies the noise $\mathbf{v} := \mathbf{W}\mathbf{n}$ at the receiver (or $\mathbf{W}\tilde{\mathbf{n}}$ in the case of precoding).

Beamforming: For the special case where $N_s = N_r = 1$, the precoder \mathbf{F} becomes a column

vector $\mathbf{f} \in \mathbb{C}^{N_t}$, $\|\mathbf{f}\|^2 = 1$ and the channel becomes a row vector. Therefore, (1) becomes:

$$y = \mathbf{h}^* \mathbf{f} x + n, \quad (6)$$

which is the reason a beamforming channel is often known as a “rank-1” channel. A well-known example of a beamforming codebook is the discrete Fourier transform (DFT) codebook. Let the codebook \mathcal{F} contain a set of these beamforming vectors \mathbf{f} , also known as “grid of beams.” Regardless of the codebook, a power-optimal beamforming precoding vector \mathbf{f}^* which maximizes the received channel gain can thus be found through a search in \mathcal{F} :

$$\mathbf{f}^* := \arg \max_{\mathbf{f} \in \mathcal{F}} |\mathbf{h}^* \mathbf{f}|^2, \quad (7)$$

which is how beamforming improves the received signal power.

The power-optimal beamforming precoder can also be computed from the channel state information if it is known at the transmitter. In this case, there is no need to search in a codebook. The optimal beamforming precoder is thus:

$$\mathbf{f}^* = \arg \max_{\mathbf{f}: \|\mathbf{f}\|^2=1} |\mathbf{h}^* \mathbf{f}|^2 = \frac{\mathbf{h}}{\|\mathbf{h}\|}, \quad (8)$$

since the quantity enclosed in the modulus operator is an inner product of the channel and the precoder vectors, which is maximized when they are both equal. This optimal beamforming precoder aligns the transmitted signal with the channel to maximize the received signal power with a gain of $\|\mathbf{h}\|^2$. Note that there is no need for a combiner in single-user beamforming, since the received signal is already a scalar quantity.

Cell-Free MIMO: Cell-free MIMO, better known by its former name coordinated multi-point (CoMP) joint transmission, exploits the phenomenon when signals transmitted from two (or more) spatially separate cells, they are likely to be strongly decorrelated and MIMO can thus take advantage of them. In this case, the large-scale fading coefficient G is redesigned so that different elements in \mathbf{H} are multiplied with different location-dependent fading coefficients based on which transmitting cell these elements represent.

Statistics:

1) Transmit power: The base station transmit power P_{total} is divided across all OFDM subcarriers and transmit antennas. Therefore, for a MIMO system with N_t transmit antennas, the average power of an OFDM subcarrier before power control is $P_x = P_{\text{total}}/N_t$.

Industry standards use the term resource element (RE) as the smallest element in an OFDM time-frequency grid corresponding to one subcarrier-symbol. In the *special* case of a single OFDM symbol, the transmit power per RE is equal to the transmit power per antenna over one OFDM symbol, which is equal to $P_x/(N_t N_{SC})$. In 4G LTE, certain REs are known as the “reference symbols” (or “reference signals” in 5G NR) and are used to estimate the channel and measure the cell coverage. If the channel gain is $\|\mathbf{H}\|_F^2$ (or $G\|\mathbf{H}\|_F^2$ with the large-scale fading as motivated earlier), then the averaged power of these reference symbols (or signals) as measured at the receiver—known as the reference signal received power (RSRP)—is $G\|\mathbf{H}\|_F^2 P_x / ((N_{\text{symb}} := 1)N_{SC})$. The path loss is the attenuation the signal undergoes as it propagates through the channel as a result of the channel impact (i.e., large-scale fading, shadowing, etc.) as shown earlier in this section. It is thus defined as $\text{PL} := G\|\mathbf{H}\|_F^2$ and is often reported in dB scale (i.e., $10 \log_{10}(\cdot)$).

2) *Signal to noise ratio*: To derive the signal to noise ratio (SNR) at the receiver, we use the system model (1) and compute the autocorrelation matrix of the received signal:

$$\begin{aligned}
 \mathbf{R}_{yy} &:= \mathbb{E}[\mathbf{y}\mathbf{y}^*] = \mathbb{E}[(\mathbf{H}\mathbf{x} + \mathbf{n})(\mathbf{H}\mathbf{x} + \mathbf{n})^*] \\
 &= \mathbb{E}[\mathbf{H}\mathbf{x}\mathbf{x}^*\mathbf{H}^*] + \mathbf{R}_{nn} \\
 &= P_x \mathbf{I}_{N_r} \mathbb{E}[\mathbf{H}\mathbf{H}^*] + \sigma_n^2 \mathbf{I}_{N_r} \\
 &\stackrel{(a)}{=} \underbrace{P_x \|\mathbf{H}\|_F^2}_{\text{signal}} + \underbrace{\sigma_n^2}_{\text{noise}},
 \end{aligned} \tag{9}$$

where (a) is a scalar quantity derived from the normalized traces of \mathbf{R}_{yy} for the ease of reading. If the SNR at the transmitter is equal to $\rho := P_x/\sigma_n^2$, and the channel gain is $\|\mathbf{H}\|_F^2$, then it follows that the SNR at the receiver before equalization is equal to $\gamma = \rho\|\mathbf{H}\|_F^2/N_f$, where N_f is the noise figure. Formally, the noise figure is the ratio of the input SNR to the output SNR at the receiver.

In the presence of an equalizer, the SNR at the receiver is different for different receive antennas due to the equalization matrix \mathbf{W} , the elements of which enhance (i.e., amplify) the noise independently as derived earlier in this section. As a result, we write the post-equalization received SNR at the j -th antenna as γ_j . Details are in Section IV.

The transmit SNR can also be written as $\rho = E_x/N_0$, where E_x is the energy of the transmitted signal and N_0 is the noise power spectral density. Given that one symbol is made of $k = \log_2 M$ bits at the transmitter, the bit energy to noise power spectral density ratio at the transmitter is

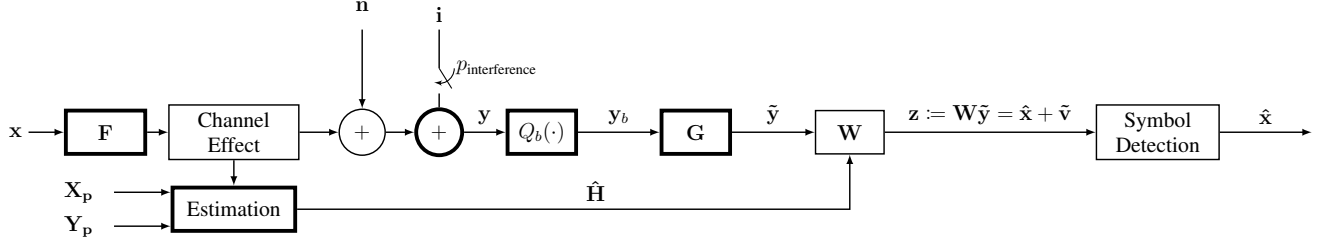


Fig. 2. A block diagram of the overall model of the wireless system (thicker boxes are optional blocks).

$E_b/N_0 = \rho/k = E_x/(kN_0)$. Note that E_b/N_0 is the per-bit SNR and that both quantities are also often represented in dB scale.

At the receiver, the bit energy to noise power spectral density ratio (E_b/N_0) post-equalization is $\gamma/(kr)$ where γ is the receive SNR and r is the code rate. The maximum code rate is defined as $r_{\max} := \mathbf{SE}/k \leq 1$. Generally, $r \leq r_{\max}$, especially as ρ decreases.

Also if the interference is present at the receiver, it is added to the noise as shown in Section IV. In this case, we have a received SINR measured per receive antenna. The total noise plus interference power is $\sigma_n^2 + p_{\text{interference}}\sigma_i^2$ as motivated in Section IV.

IV. MODEL-DRIVEN IMPLEMENTATION

We start with the implementation of various functions of wireless network through models and statistics as shown in Fig. 2. We call this “model-driven” as opposed to “data-driven” which is discussed later in Sections V, VI, and VII. A b -bit quantizer is denoted as $Q_b(\cdot)$ and is optional. We use $\mathbf{W} \in \mathbb{C}^{N_r \times N_t}$ as a channel equalizer, which removes the effect of the channel onto the received data. However, equalizers require an estimate of the channel state information, which the receiver computes at its end. This estimate is denoted as $\hat{\mathbf{H}}$ and has the same dimensions as \mathbf{H} . Channel estimation is enabled through “pilots” which are a sequence known to both the transmitting and receiving ends of the wireless system. Pilot symbols and cyclic prefix (CP) symbols (seen in both 4G LTE and 5G) are not the same—pilot symbols are used to estimate the channel and CP serves two purposes: (1) reduces inter-carrier interference and (2) allows the use of circular convolution which translates to a multiplication operation in the frequency domain.

Constellation: We follow the notation of [3] in generating the symbols for both QPSK and M -QAM as baseband symbols. For QPSK, the inphase (I) and quadrature (Q) branches take

the values ± 1 and for M -QAM they take values in the integer interval $[-\sqrt{M} + 1, \sqrt{M}]$. These constellation symbols are normalized so the power per symbol is equal to unity and are Gray-coded as stated earlier. Let the constellation be a set \mathcal{C} . This constellation has a cardinality $|\mathcal{C}| = M$.

Noise: At the receiver, the noise signal is a complex zero-mean Normal random variable with a variance (or noise power) of $\sigma^2 := k_B T \Delta f N_f$, where k_B is the Boltzmann constant, T is the temperature in Kelvins and N_f is the noise figure at the receiver, as mentioned earlier.

Interference: Besides the channel effect that brings interference through the off-diagonal elements on \mathbf{H} (i.e., the coupling between different transmit-receive antenna pairs), another method to model interference across all subcarriers is a binomial random variable with a probability of a receive antenna interfered at being $p_{\text{interference}}$. If we represent the interference signal as an independent and identically sampled from a zero-mean complex Normal random variable with $\sigma_i^2 = P_{\text{interference}}$ in a similar to the noise, then the additive interference per OFDM subcarrier is a column vector with the dimension $\mathbf{i} \in \mathbb{C}^{N_r}$ that contains either zeros or an interference signal. Hence, the average interference power is equal to $p_{\text{interference}} \sigma_i^2$ across all OFDM subcarriers.

Codeword Construction: We generate a random sequence of bits as a payload. The maximum size of this payload in bits is $L_{\text{codeword}}^{(\max)} = k N_{\text{SC}} N_t$ (or $k N_{\text{SC}} N_s$ in the case of SM) transmitted over a duration of one OFDM symbol. The cyclic redundancy check (CRC) polynomial generator function $\mathcal{P}(\mathbf{x})$ operates on this payload and adds an overhead equal to the CRC length in bits. There is only one CRC sent per transmission, regardless of the channel transmission rank and it is positioned at the end of the transmission block (i.e., the codeword). The receiver extracts the CRC and attempts to compare it with a fresh CRC computed on the received block for a match. If either the payload or the CRC does not occupy an integer number of symbols, padding is necessary. Hence, a codeword is a payload, a variable padding length, and a CRC.

Padding: If the CRC length in bits is equal to L_{CRC} , then the CRC length (in bits) with padding included is $k \lceil L_{\text{CRC}}/k \rceil$. Moreover, if the payload size is L_{payload} , then a similar formula can be derived for the payload. However, what remains is the variable padding length. To compute this padding length, we solve a non-convex optimization problem:

$$\begin{aligned}
\text{minimize:} \quad & L_{\text{padding}} \\
\text{s.t.:} \quad & L_{\text{codeword}} := L_{\text{payload}} + L_{\text{padding}} + L_{\text{CRC}} \geq 0, \\
& L_{\text{codeword}} \equiv 0 \pmod{N_t}, \\
& L_{\text{codeword}} \equiv 0 \pmod{N_{\text{SC}}}, \\
& L_{\text{codeword}} \leq L_{\text{codeword}}^{(\max)}.
\end{aligned} \tag{10}$$

Other techniques such as forward error correction (FEC) and bit interleaving can also be used in constructing the payload, making it more robust against channel impairments. Common examples of FEC are turbo codes and low-density parity check (LDPC) codes—none of which is implemented in the source code today.

Quantization: Mapping continuous and infinite values that \mathbf{y} takes to a smaller set of discrete finite values makes it easier to group symbols that “appear” similar and treat them like so—greatly reducing computational overheads (e.g., in machine learning). However quantization is irreversible, non-linear, and causes a degradation to the quality of these symbols known as the “distortion”. Therefore, employing a quantizer comes with its drawbacks and designs may avoid it. We use a truncation quantizer and define a b -bit quantization function as $Q_b(\cdot)$, with b being the quantization resolution. This quantizer thus has 2^b quantization levels.

Channel Estimation: Let the pilot symbols have a length n_{pilot} OFDM symbols. We denote the fat matrix of known pilot symbols $\mathbf{X}_{\text{P}} \in \mathbb{C}^{N_t \times n_{\text{pilot}}}$. Note that this matrix cannot be tall because the number of pilots must at least be equal to the number of transmit antennas ($n_{\text{pilot}} \geq N_t$). Let the received pilot symbol values (i.e., channel response) be stored in another matrix $\mathbf{Y}_{\text{P}} \in \mathbb{C}^{N_r \times n_{\text{pilot}}}$. Then we can compute the least-squares (LS) estimate of the channel as follows:

$$\hat{\mathbf{H}}_{\text{LS}} = \arg \min_{\mathbf{H}} \|\mathbf{Y}_{\text{P}} - \mathbf{H}\mathbf{X}_{\text{P}}\|^2, \tag{11}$$

which—besides the traditional way of writing the norm as an inner product—can be solved as follows:

$$\begin{aligned}
\mathbf{Y}_{\text{P}} &= \hat{\mathbf{H}}\mathbf{X}_{\text{P}} \\
\mathbf{Y}_{\text{P}}\mathbf{X}_{\text{P}}^* &= \hat{\mathbf{H}}\mathbf{X}_{\text{P}}\mathbf{X}_{\text{P}}^* \\
\mathbf{Y}_{\text{P}}\mathbf{X}_{\text{P}}^*(\mathbf{X}_{\text{P}}\mathbf{X}_{\text{P}}^*)^{-1} &= \hat{\mathbf{H}} \\
\hat{\mathbf{H}} &= \mathbf{Y}_{\text{P}}\mathbf{X}_{\text{P}}^*(\mathbf{X}_{\text{P}}\mathbf{X}_{\text{P}}^*)^{-1}.
\end{aligned} \tag{12}$$

There is a little abuse of notation in the derivation above since the pilot symbols and the channel response are matrixes.

Pilot Design: Since the matrix \mathbf{X}_P is not square, it should be carefully designed so that $\mathbf{X}_P \mathbf{X}_P^*$ is invertible. An example of carefully designed codes is Zadoff-Chu codes in both 4G LTE and 5G. However, for simplicity we exploit the idea of semi-unitary matrixes such that $\mathbf{X}_P \mathbf{X}_P^* = \mathbf{I}_{N_t}$ and therefore we do not need to worry about the invertibility of $\mathbf{X}_P \mathbf{X}_P^*$ any further. At a high level, the construction of a unitary matrix (i.e., $\mathbf{Q}^{-1} = \mathbf{Q}^*$) is possible through either DFT, a QR decomposition of a matrix the elements of which are sampled from $\mathcal{N}_{\mathbb{C}}(0, 1)$, or a combinatorial rearrangement of orthonormal bases.

Consequently, the LS channel estimate $\hat{\mathbf{H}}$ from (12) becomes:

$$\hat{\mathbf{H}}_{\text{LS}} = \mathbf{Y}_P \mathbf{X}_P^* \quad (13)$$

The linear MMSE estimation (LMMSE) minimizes the mean squared error in the channel estimate and is thus written as

$$\hat{\mathbf{H}}_{\text{LMMSE}} := \arg \min_{\hat{\mathbf{H}}: \hat{\mathbf{H}} = \mathbf{A}\mathbf{y}} \mathbb{E}[\|\mathbf{H} - \hat{\mathbf{H}}\|_F^2] \quad (14)$$

where $\hat{\mathbf{H}} = \mathbf{A}\mathbf{y}$ is a *linear* transform (hence the qualifier “linear”). Solving for the Frobenius norm as the trace of an outer product and finding the gradient of the mean squared error with respect to \mathbf{A} then setting it to $\mathbf{0}_{N_r \times N_t}$, we obtain the LMMSE for a given transmit SNR and the channel covariance matrix $\mathbf{R}_{\mathbf{H}\mathbf{H}}$:

$$\hat{\mathbf{H}}_{\text{LMMSE}} = \mathbf{R}_{\mathbf{H}\mathbf{H}} \left(\mathbf{R}_{\mathbf{H}\mathbf{H}} + \frac{1}{\rho} \mathbf{I}_{N_r} \right)^{-1} \hat{\mathbf{H}}_{\text{LS}}. \quad (15)$$

Note that this channel covariance (or precisely, correlation) matrix can be found from the time-based averaging of the quantity $\mathbf{H}\mathbf{H}^*$). Due to LMMSE having prior knowledge of the channel statistics as evident from the channel covariance matrix above, it outperforms LS estimation.

Channel Equalization: As mentioned earlier, channel equalization intends to remove the impact that the channel made onto the transmitted symbols. Two commonly used types of channel equalizations are (1) zero-forcing (ZF) and (2) minimum mean square error (MMSE) equalization. Let us call the equalizer \mathbf{W} which is computed from a given channel (either perfectly known or estimated). Further, let us continue to use the SM type of MIMO and thus

apply the equalizer to the diagonalized channel Σ system as shown in (4). In this case:

$$\begin{aligned}\tilde{\mathbf{z}} &:= \mathbf{W}\tilde{\mathbf{y}} = \mathbf{W}\Sigma\mathbf{s} + \mathbf{W}\tilde{\mathbf{n}} \\ &= \hat{\mathbf{x}} + \tilde{\mathbf{v}}.\end{aligned}\tag{16}$$

If we denote an estimated channel—regardless whether precoded or not—as $\hat{\mathbf{H}}$ then the ZF equalizer of this estimated channel is given by:

$$\hat{\mathbf{x}} = \arg \min_{\mathbf{x}} \|\mathbf{y} - \hat{\mathbf{H}}\mathbf{x}\|^2 = \mathbf{H}^\dagger \mathbf{y},\tag{17}$$

from which we deduce from (16) that $\mathbf{W}_{\text{ZF}} = \mathbf{H}^\dagger$. Three immediate cases emerge from the pseudo-inverse: First, if the channel $\hat{\mathbf{H}}$ is square and invertible (i.e., full rank), then $\mathbf{W}_{\text{ZF}} = \mathbf{H}^{-1}$. Second, if the channel is wide (or $N_t > N_r$) and has full row rank, then $\mathbf{H}^\dagger = \mathbf{H}^*(\mathbf{H}\mathbf{H}^*)^{-1}$. Finally, if the channel is tall (or $N_t < N_r$) and has full column rank, then $\mathbf{H}^\dagger = (\mathbf{H}^*\mathbf{H})^{-1}\mathbf{H}^*$. This pseudo-inverse (i.e., in (17)) becomes a concern if the channel matrix is ill-conditioned (e.g., close to singular)[‡].

For ZF equalization, keeping in mind that $\mathbf{R}_{\mathbf{x}\mathbf{x}} = P_x \mathbf{I}_{N_t}$ and $\mathbf{R}_{\mathbf{n}\mathbf{n}} = \sigma_n^2 \mathbf{I}_{N_r}$, the post-equalization SNR on the j -th decoded stream γ_j^{ZF} is

$$\gamma_j^{\text{ZF}} = \rho \frac{1}{[\mathbf{W}\mathbf{W}^*]_{j,j}} = \rho \frac{1}{[(\hat{\mathbf{H}}^*\hat{\mathbf{H}})^{-1}]_{j,j}}.\tag{18}$$

The construct $[\mathbf{A}]_{j,j}$ means the j -th diagonal element of the matrix \mathbf{A} . ZF equalization completely eliminates the interference due to the coupling between different transmit-receive antenna pairs, hence the name. Due to the concerns in the pseudo-inverse formula as outlined earlier, an alternative equalization technique is considered.

The MMSE equalizer of the estimated channel minimizes the residual error term:

$$\mathbf{W}_{\text{MMSE}} = \arg \min_{\mathbf{W}} \mathbb{E}[\|\mathbf{W}\mathbf{y} - \mathbf{x}\|^2],\tag{19}$$

which when introducing the trace operator, computing the gradient, and setting it to $\mathbf{0}_{N_t \times N_r}$, we

[‡]Matrix inversion—even for well-conditioned matrixes—is a computationally expensive operation, especially with the increasing deployment of massive MIMO in later 5G releases which creates a larger dimension \mathbf{H} . This justifies the need for graphics processing units.

obtain:

$$\begin{aligned}\mathbf{W}_{\text{MMSE}} &= \mathbf{R}_{\mathbf{xy}} \mathbf{R}_{\mathbf{yy}}^{-1} \\ &= \hat{\mathbf{H}}^* (\hat{\mathbf{H}} \hat{\mathbf{H}}^* + \frac{1}{\rho} \mathbf{I}_{N_t})^{-1}.\end{aligned}\quad (20)$$

Similarly, the average post-equalization SNR per antenna on the j -th decoded stream due to the MMSE equalization equals

$$\gamma_j^{\text{MMSE}} = \rho \frac{1}{[\mathbf{W}\mathbf{W}^*]_{j,j}}, \quad (21)$$

which can also be derived in terms of the channel estimate $\hat{\mathbf{H}}$ (for the eager reader).

At low SNRs, ZF further amplifies the noise and thus MMSE offers as a useful advantage at low SNR. However, at high transmit SNRs (i.e., $1/\rho \rightarrow 0$), the MMSE functions just as well as a ZF equalizer since it approaches a matrix inverse. Otherwise, the MMSE equalizer does not lead to complete elimination of the interference [4].

Another equalization technique uses the maximum likelihood receiver to decode the received vector \mathbf{y} . It does so by exhaustively searching for a vector of symbols (needing up to $|\mathcal{C}|^{N_t}$ searches) that *maximizes* the likelihood of the noise random variable (i.e., Gaussian), or:

$$\hat{\mathbf{x}} = \arg \min_{\mathbf{x}} \|\mathbf{y} - \hat{\mathbf{H}}\mathbf{x}\|^2. \quad (22)$$

This equalization technique is SNR-optimal in the sense of no losses in the per-antenna SNR.

Symbol Detection: The last step is to convert the received symbols to the symbols belonging to the constellation. Since \mathbf{v} is also Gaussian, we can use a maximum likelihood detector (or k -means clustering as detailed later). In this case, every symbol in \mathbf{z} , which we call $z \in \mathbb{C}$, can be found based on the Euclidean distance from the nearest symbol in the constellation $\{s_m\}_{m=0}^M$. Thus we obtain a column vector $\hat{\mathbf{m}}^*$ from \mathbf{z} , which is comprised of the entries \hat{m}^* that fulfill the following relationship:

$$\hat{m}^* = \arg \min_m |z - s_m|, \quad m \in \{0, 1, \dots, M-1\}. \quad (23)$$

Furthermore, since every m corresponds to one I/Q symbol, we can also obtain the column vector $\hat{\mathbf{x}}$ the entries of which are the detected symbols. Because every symbol represents a string of bits, the received codeword (including the padding and the CRC) can be recovered from $\hat{\mathbf{x}}$ for further analysis.

So far we have covered model-driven applications of Python in wireless communications.

Namely: construction of symbols, creation of a MIMO payload with CRC, creation of a channel, creation of additive noise, estimation of the channel using pilots, channel equalization, and symbol detection. Next, we focus on a data-driven approach where the value of machine learning and artificial intelligence is demonstrated. Three areas of interest are: unsupervised learning, supervised learning (including deep learning), and reinforcement learning.

V. UNSUPERVISED MACHINE LEARNING USE CASES

A. Clustering

The use of k -means clustering[§] to perform symbol detection is the quintessential application of unsupervised learning in wireless communications. In the code implementation of this case, a two-dimensional plane representing the I/Q components of the complex-valued symbols is formed. The k -means centroids \mathcal{C} are initialized (and fixed) to these M constellation symbols (this is a major difference from the common k -means algorithm). Then a two-dimensional column vector \mathbf{z} is constructed from the received symbols $z := z_I + jz_Q$ as follows $\mathbf{z}^\top := [z_I, z_Q]$. The centroids in \mathcal{C} are constructed in a similar fashion. Next, the symbols in presence of additive noise are grouped in a way that minimizes the Euclidean distance to a centroid:

$$m^* = \arg \min_{\mathbf{c} \in \mathcal{C}: |\mathcal{C}|=M} \|\mathbf{z} - \mathbf{c}\|. \quad (24)$$

which is essentially similar to the result from (23).

B. Kernel Density Estimation

The kernel density estimation (KDE) is a nonparametric estimate of a given density of a random variable through a group of kernels and smoothing parameters (or bandwidths). Let us take the conditional density $f(\mathbf{y} \mid \mathbf{H}, \mathbf{x})$. This density is equal to $f_{\mathbf{n}}(\mathbf{y} - \mathbf{H}\mathbf{x}) = \mathcal{N}_{\mathbf{C}}((\mathbf{y} - \mathbf{H}\mathbf{x}), \sigma_n^2 \mathbf{I}_{N_r})$. However, with the introduction of the quantizer, the density is no longer Gaussian since quantization is a non-linear operation. To estimate the density in presence of the quantizer $f(\mathbf{y}_b \mid \mathbf{H}, \mathbf{x})$, either (1) an *empirical* density can be constructed (i.e., through binning intervals, counting of samples per bin, and then dividing by the total), which does not introduce any density biases (though the number of bins can be a subjective choice) or (2) KDE can be applied which uses a kernel function (e.g., a Gaussian mixture) to generate a smooth curve.

[§]The k and the \mathcal{C} in k -means here should not be confused with the k and the \mathcal{C} defined in Section III which represent the number of bits per symbol in a constellation \mathcal{C} of size M .

Finding an optimal number of bins to fit an empirical density can be an arduous task and defending it later can be challenging due to the subjectivity. Thus, resorting to a nonparameteric estimate of the density through KDEs has become more convenient[¶].

Further Use Cases: In unsupervised learning, here are a few use cases: anomaly detection and root cause analysis through clustering [5], quantization using k -means, and wireless fingerprinting (i.e., distinguishing between devices sending similar messages) or localization using clustering algorithms [6].

VI. SUPERVISED MACHINE LEARNING USE CASES

We define the learning task of supervised machine learning using a matrix of inputs in a design matrix format \mathbf{X} , a supervisory signal of a column vector \mathbf{y} , the predicted supervisory signal of a column vector $\hat{\mathbf{y}}$, and a set of hyperparameters Θ . The multi-dimensional space spanned by the columns of \mathbf{X} define the feature space. The full data matrix is $\mathbf{M} := [\mathbf{X} \mid \mathbf{y}]$. To avoid confusion with the model-based development in Section IV, any symbol used moving forward is expected to refer to this terminology unless explicitly referred to an equation from Section IV.

Formally, a supervised learner minimizes a loss function $L(\mathbf{y}, \hat{\mathbf{y}}; \Theta)$ through a search space defined by the hyperparameters. An optimizer uses the training dataset to find the optimal Θ^* and the validation set is used as a benchmark to report on the loss function. Formally:

$$\underset{\Theta}{\text{minimize:}} \quad L(\mathbf{y}, \hat{\mathbf{y}} := f_{\Theta}(\mathbf{X}); \Theta), \quad (25)$$

where $f_{\Theta}(\mathbf{X})$ is a supervised learning model specific function. Depending on the data type that \mathbf{y} represents, we could have a “regressor” for continuous supervisory data $[\mathbf{y}]_i \in \mathbb{R}$ (an example of which would be an estimate of the channel state information \mathbf{H} or a “classifier” for categorical supervisory data $[\mathbf{y}]_i \in \mathbb{Z}$, where the class labels have no quantitative significance (such as the beam identifier or the transmit antenna identifier). Examples of optimizers that are used extensively today are the stochastic gradient descent (SGD) and the adaptive moments (Adam). Details on SGD and Adam can be found in [7].

The process through which wireless systems data is obtained and training is performed is elaborate. However, in short, there are two common approaches today: (1) *learn-exploit-invalidate* where the base station obtains data from a group of users it serves for a period of time and then

[¶]Well, there are some of parameters that can be adjusted in KDEs.

it trains the model for another period of time (defined by a duty cycle), after which the model is used for an exploitation period (i.e., inference) until the performance falls below a certain threshold, after which the model is invalidated and the cycle repeats and (2) *periodic transfer learning* where training happens periodically at a central location (base stations either stream actual data to it) or by federated learning (where each base station only shares the deep learning weights it has computed locally and the serving base station aggregates these local updates).

There are several machine learning algorithms that can be used. However, to make this brief and relevant, we choose two algorithms: linear regression and deep learning. Also, we only provide detail for a single wireless communications use case each to avoid overwhelming the reader with too much information.

A. Linear Regression

Channel Estimation: Let us take the case of a MIMO system with two transmit antennas and two receive antennas (i.e., a 2×2 channel). In such a case, we can write (1) using real-valued scalar variables as:

$$\begin{aligned} y_1 &= h_{11}x_1 + h_{12}x_2 + n_1 \\ y_2 &= h_{21}x_1 + h_{22}x_2 + n_2 \end{aligned} \tag{26}$$

which means that we could learn h_{11}, h_{12} using x_1, x_2 and y_1 as learning features. Similarly we could learn h_{21}, h_{22} using x_1, x_2 and y_2 as learning features. The linear regression problem thus becomes $y_1 = \mathbf{h}_1^\top \mathbf{x} + \epsilon_1$, with ϵ_1 sampled from a Gaussian distribution and \mathbf{h}_1 being a column vector representing the respective elements of the channel. In other words, to learn the column vector $\mathbf{h}_1^\top := [h_{11}, h_{12}]$, we need to construct a data matrix of measurements in the format $\mathbf{M} \in \mathbb{R}^{N_{sc} \times 3} := [x_1, x_2 \mid y_1]$. This is repeated for the imaginary part and the remaining signal elements in \mathbf{y} . It can also be generalized for systems other than 2×2 .

B. Deep Learning

Deep neural networks (DNN) have been used successfully to perform various wireless communications procedures. Let our DNN have a depth D and width W . Since the majority of variables in wireless communications can be normalized (or scaled in the interval $[0, 1]$), the non-linear activation function $f(\cdot)$ can be the sigmoid function, while other choices of an activation function such as the rectified linear unit can also be considered especially if certain variables

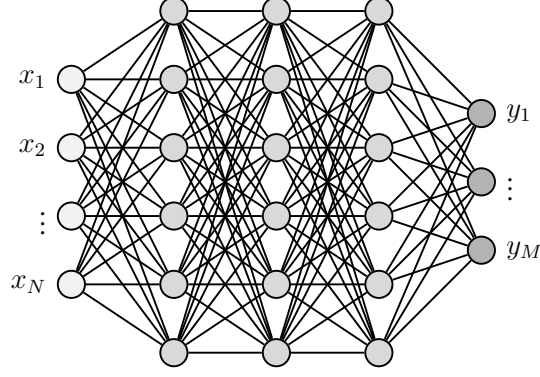


Fig. 3. Fully connected deep neural network (depth $D = 3$ and width $W = 6$) of an input N and an output M .

are not scaled. If every node in one layer is connected to every node in the next layer, the DNN is known as a fully connected DNN, as in Fig. 3.

Symbol Detection: Let us study the case where we would like to perform symbol detection from a constellation of size M in the presence of noise. The learning features thus are the various I/Q symbols \mathbf{x} and the symbol identifier $\{0, 1, \dots, M - 1\}$. If we separate the real \mathbf{x}_r and imaginary part \mathbf{x}_i of these symbols into two column vectors, we thus have a full data training matrix of $\mathbf{M} \in \mathbb{R}^{M \times 3} := [\mathbf{X} := [\mathbf{x}_r, \mathbf{x}_i] \mid \mathbf{y}]$. However, for inference there are more number of symbols to label than the constellation size itself. As a result, we have to increase the size of the training dataset. Otherwise, the model is very likely to underfit (overfitting and underfitting are not discussed in this primer). To make the model more robust, we introduce Normal distributed noise to \mathbf{X} and repeat the same supervisory labels \mathbf{y} for an augmented data matrix $\tilde{\mathbf{M}} \in \mathbb{R}^{qM \times 3}$, with q being a small positive integer as a result of this perturbation step. This leaves us with a data *inference* matrix $\mathbf{M} \in \mathbb{R}^{N_{sc}N_r \times 3} := [\text{Re}[\mathbf{y}], \text{Im}[\mathbf{y}] \mid \mathbf{m}]$ which is constructed from all the data points from all receive antennas as in Section III. If a split for training and test data is required for the augmented data matrix, it must be large enough for the random split not to ruin the adequate representation of symbol identifiers.

Given the nature of the supervisory signal (i.e., representing categories that do not have any quantitative significance), it is encoded into a binary class matrix for both the training and inference data matrixes. Thus, a softmax activation function at the output layer of the DNN and a categorical cross-entropy loss function are required.

Loss functions: Loss functions (25) are what the deep learning optimizer aims at minimizing. Examples of loss functions are the (root) mean squared error or the mean absolute error are both

used to measure how far the predicted supervisory signal $\hat{\mathbf{y}}$ is from the true supervisory signal \mathbf{y} . Mathematically, $\text{MSE} := \frac{1}{M} \sum_{i=1}^M ([\hat{\mathbf{y}}]_i - [\mathbf{y}]_i)^2$ and $\text{MAE} := \frac{1}{M} \sum_{i=1}^M |[\hat{\mathbf{y}}]_i - [\mathbf{y}]_i|$. To keep track of the performance of a model as a result of optimizing the loss, performance measures, known as metrics, are reported.

Equalization and Detection in a Rotation Channel: Let there be a channel the task of which is to rotate complex-valued OFDM subcarriers by an angle θ and add some noise (which may not necessarily be Gaussian). In other words, for ν transmitted OFDM subcarriers, we have a system model: $\mathbf{y} = e^{j\theta} \mathbf{I}_\nu \mathbf{x} + \mathbf{n}$. Given that these symbols have a spatial relationship with one another, as known from their I/Q constellation, the use of convolutional neural networks (CNNs) may help recover \mathbf{x} from \mathbf{y} . In other words, we train the CNN to perform the channel equalization and symbol detection together.

CNNs: CNNs have the ability to discern spatial relationships between learning features. Because of that, if we construct the learning features such that the training data $\mathbf{M} \in \mathbb{R}^{\nu \times 4} := [\mathbf{X} \mid \mathbf{y}] = [\text{Re}(\mathbf{y}), \text{Im}(\mathbf{y}) \mid \text{Re}(\mathbf{x}), \text{Im}(\mathbf{x})]$, then a CNN can likely exploit the spatial relationship between the real and imaginary part of both the input and output symbols through the use of convolutional layers with kernel sizes equal to the number of learning features in \mathbf{X} , which equals 2. Also, to capture any spatial relationship across symbols, we set the stride value to 1 so the kernel moves one symbol component per convolution step. CNNs can also be useful in problems related to multi-user beamforming strategies for massive MIMO, reflective intelligent surfaces, scheduling, and more.

Reproducibility: Unlike the feedforward deep neural networks, CNNs have issues related to reproducibility, even with the seed being fixed. Therefore, it is a good practice to save the model weights once a satisfactory result is obtained.

Beam Prediction in Trajectory: If a user's trajectory follows a street or any path with many users on it, then the construction of a time series that can predict the next SINR-optimal beam from a codebook of beamforming vectors (or a grid of beams) becomes a possibility through the use of recurrent neural networks (RNNs). RNNs can process sequential data and are thus suitable for time series. We examine the long short-term memory (LSTM) type of RNN here.

LSTMs: LSTMs can remember information for an extended period larger than that of RNNs, making them suitable for our problem. LSTMs comprise multiple elements: (1) memory cell state, which is generally common in RNNs (2) forget gate and (3) input gate. The memory cell states simply record information. The input gate is used to update the memory cell state.

The forget gate can learn to reset the state of the memory cell when the stored information is no longer needed (i.e., invalidation of the memory cell). If we denote vectors of the candidate memory cell (i.e., new information) as $\tilde{\mathbf{c}}_t$, the forget gate as \mathbf{f}_t , the input gate as \mathbf{i}_t , then we can represent the impact of the forget and input gate on the memory cell output as follows:

$$\mathbf{c}_t := \mathbf{c}_{t-1} \odot \mathbf{f}_t + \tilde{\mathbf{c}}_t \odot \mathbf{i}_t.$$

Feature engineering: Feature engineering for time series can be in general a bit tricky compared to regression or classification that is not time-based. Let our full data matrix be $\mathbf{M} := [\mathbf{X} \mid \mathbf{y}]$ which captures historical data of N learning features over T time steps, each time step has M records. Thus, $\mathbf{M} \in \mathbb{R}^{MT \times N}$. Specifically, for beam prediction \mathbf{X} captures the time stamp, the user identifier, the received power, and the received SINR. Optionally, it can also include the longitude and latitude coordinates of each user. These dictate the dimension of the learning features N . Also, \mathbf{y} is the target variable that captures the beam identifier corresponding to the highest SINR at that *time* for that user. With a sufficiently explained \mathbf{M} , we quickly go over a few feature engineering techniques suitable for time series to improve the predictability:

- 1) **Shifting and Lagging:** A timeshift is applied block-wise with past and future shift values on \mathbf{M} . That is, the dataset becomes $[\mathbf{M}_{t-k} \mid \dots \mid \mathbf{M} \mid \dots \mid \mathbf{M}_{t+\ell}]$, with k and ℓ being the lag and lead shifts respectively. The lead time ℓ defines the prediction horizon which is how many time steps in the future is the LSTM expected to predict. This shifting and lagging operation leads to an additional $k + \ell$ columns in the dataset. The undefined values as a result of these operations can be filled with the last known value to avoid reducing row count.
- 2) **Differencing:** The differencing operation reduces trend in the time series and makes the series more stationary. Let us define the j -th order difference as a column vector $\Delta_{t-j} := \mathbf{x}_t - \mathbf{x}_{t-j}$, $j \in \{1, 2, 3, \dots, N\}$ and apply it column-wise on the learning features $[\Delta_{t-k} \mid \dots \mid \mathbf{0} \mid \dots \mid \Delta_{t+\ell}]$.

Thus an engineered data matrix $\tilde{\mathbf{M}}$ is constructed as

$$\tilde{\mathbf{M}} := [\Delta_{t-k} \mid \mathbf{M}_{t-k} \mid \dots \mid \mathbf{0} \mid \mathbf{M}_t \mid \dots \mid \Delta_{t+\ell} \mid \mathbf{M}_{t+\ell}], \quad (27)$$

which is a matrix in $\mathbb{R}^{MT \times (2N(k+\ell)+1)}$. This matrix is then partitioned into $\tilde{\mathbf{M}} = [\mathbf{X} \mid \mathbf{y}_\ell]$, with \mathbf{y}_ℓ

being the beam identifier at a single future lookahead value^{||} equal to the prediction horizon of interest (also known as the “offset”) ℓ . These partitions are further converted into tensors having the shape (timesteps, record, and features).

There are more feature engineering techniques that can further be applied to time series. For example, besides the scaling part (which we have mentioned earlier) and applying $\log(\cdot)$ to positive-valued features, the application of FFT onto a learning feature $x(t)$ extract frequencies that have high information content (e.g., as measured by the power spectral density $|X(f)|^2$) can be often useful. In particular, in transforming the learning feature to a sinusoid $\varphi_k: x(t) \mapsto \cos(2\pi f_k x(t))$, FFT can help determine which frequencies f should be used in constructing this transformation. There are some nuances with using FFTs: First, if the periodicity of this signal $x(t)$ is T_s , then the frequency of this signal is $1/T_s = F_s$. Also, if the signal is aperiodic, then a window function can be applied first. Second, if the FFT has N_{FFT} points, then $\Delta f := F_s/N_{\text{FFT}}$. Third, the computation of $f_k = k\Delta f, k \in \{0, 1, \dots, N_{\text{FFT}} - 1\}$ which corresponds to the frequencies in the interval $[-F_s/2, F_s/2]$. Finally, plotting the power spectral density versus frequency provides an indication which frequencies f_k have the highest information content and thus should be used in the transformation φ_k (there could be several suitable k 's).

Training-test split: Different from random splitting, a time series split of the engineered data matrix $\tilde{\mathbf{M}}$ has two types of constraints it has to fulfill: (1) no randomness hence the sequence (order of data within column vectors) is undisturbed and (2) the split must abide by the time boundaries (e.g., if the measurements are over a radio frame, then splits can only happen at the boundary of whole radio frames). Therefore, for a training split ratio r_{training} , the first $\lfloor \lfloor r_{\text{training}} MT \rfloor / T \rfloor T$ rows belong to the training set while the remainder belongs to the test dataset. Notice that we cannot set r_{training} arbitrarily as it has a time boundary it is adjusted to.

Reproducibility: Similar to CNNs, LSTMs also have problems with reproducibility.

Channel State Information Compression: Since different OFDM subcarriers experience correlated fading despite the different frequencies [8], [9], applying parts of the CSI towards other OFDM subcarriers while removing redundant other parts or even exploiting the channel sparsity (i.e., effectively “compressing” the channel) is beneficial in reducing the control plane overhead, especially for users that are in high SNR environments. The compression ratio $0 \leq \kappa < 1$ is the ratio that determines the latent layer dimension and is agreed upon by both the UE and BS:

^{||}Actually, forecasting multiple time steps is also possible either as a single shot or through an autoregressive approach where one prediction is made at a time and then fed back to the model.

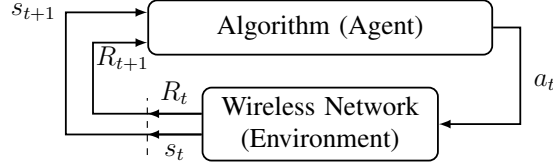


Fig. 4. Actions, states, and rewards: reinforcement learning.

A smaller latent dimension enables transmission of less bits. The UE compresses the channel using the encoder to a dimension $D := N_r N_t [(1 - \kappa) N_{SC}]$ while the BS decompresses it and reconstructs the CSI—with loss—using the decoder.

Autoencoders: Deep autoencoders are a “self-supervised” learning technique that uses deep neural networks to efficiently learn how to compress and encode data. They then learn to reconstruct the data back from the compressed encoded representation to another that is close to the original input (hence self-supervised). Autoencoder compression is a lossy compression technique since the reconstructed data is not equal to the original. Autoencoders are comprised of three different layers: an encoder, a latent layer, and a decoder.

Further Use Cases: In supervised learning, other types of learners not covered in this primer release can be explored such as ensemble learners. Additionally, more use wireless cases can be explored such as predicting inter-band handover success [10], [11] which has today become 3GPP Rel-16 conditional handovers, signal denoising using autoencoders, improving the conditions in which joint transmission can be triggered in CoMP [12] or cell-free MIMO, and predicting an optimal transmit beam per users in a trajectory using LSTMs [13].

VII. REINFORCEMENT LEARNING USE CASES

In the case where training data is not in a data matrix format (or simply unavailable), a policy (e.g., of a game) can be used to train an agent to “win” by learning a reward-maximizing policy. A policy $\pi(\cdot | \cdot)$ maps the state-action space to a probability from the vantage point of the agent. Formally:

$$\pi(a \in \mathcal{A} | s \in \mathcal{S}) := \mathbb{P}[A = a | S = s] : \mathcal{S} \times \mathcal{A} \rightarrow [0, 1]. \quad (28)$$

In reinforcement learning, an agent (an algorithm) interacts with the environment (a wireless network) through an action $a \in \mathcal{A}$ at a time step t towards the environment for the environment to return an instantaneous reward $R \in \mathbb{R}$ in return and move into a new observation state $s \in \mathcal{S}$

as a result of this action. This interaction is outlined in Fig. 4. To formulate a problem as a reinforcement learning problem, a Markov decision process (MDP) is defined. MDPs are a tuple of five elements: actions, states, rewards, probability of state transitions as observed by the environment, and a reward discounting factor. MDPs assume the Markov property: The future state s' depends only on the current state s and action a and not on the sequence of past states (i.e., memoryless). Therefore, the probability of state transitions is $\mathbb{P}[S' = s' \mid S = s, A = a]$.

Since the true policy $\pi(\cdot \mid \cdot)$ is not always revealed or known, an “off-policy” algorithm known as Q -learning [14] is used to implicitly learn the true policy or find the optimal action-value function for the policy π written as $Q_\pi^*(s, a)$. This can be done through several ways, but the ϵ -greedy method is popular. In this approach, a choice between exploration (random search) and exploitation (reuse of learning) is made with a probability ϵ , which is decayed every new learning episode as the agent learns more about the environment, making exploration less likely. During every episode, the Q -learner improves its “experience” as measured by the action-value function $Q_\pi(s, a)$. The ultimate goal is for Q -learning to learn an optimal representation of the policy. That is, find $Q_\pi^*(s, a)$ which represents an optimal strategy to choose an action a' that maximizes the expected future discounted reward given the current state s and action a . Mathematically:

$$Q_\pi^*(s, a) = \mathbb{E}_{s'}[R + \gamma \max_{a'} Q_\pi^*(s', a') \mid s, a], \quad (29)$$

where R is the present reward and $0 < \gamma < 1$ is the reward discounting factor. This is known as the Bellman equation.

To solve this equation and compute this expectation, there are two approaches: One approach does this iteratively and hopes that as $i \rightarrow +\infty$ that $Q_i(s, a) = Q^*(s, a)$. Another approach uses a deep neural network as a universal function approximator and trains it so that $Q(s, a; \Theta) = Q_\pi^*(s, a)$. This is the essence of Q -learning with deep neural networks, also known as the deep Q -network (DQN). The difference between the action-value function at time t and that of the optimal action-value function is known as the “regret.” In other words, the regret at the i -th time instant is $Q^*(s, a) - Q_i(s, a)$ and as $i \rightarrow +\infty$, regret should ideally approach zero.

Thus, there are two flavors of Q -learning used today: tabular and deep. We will focus our development only on DQNs. The reason is because for the tabular Q -learning to function as desired, a discretization of the observation space into bins is necessary so one state represents vectors to bin indexes. This prevents a good isolation between the agent and environment classes,

since the agent has to be *explicitly* aware of the environment bounds. Thanks to neural networks, the vector of states can be used to train (and later infer) the “best” action without explicitly learning about these environment bounds.

While optimizing the loss function, neural networks can be stuck in local minima, oscillate, or even diverge. This is why the idea of sampling experience from a replay buffer that stores the tuple (s_t, a_t, R_t, s_{t+1}) obtained at time t can help since the behavior distribution is averaged over many of its previous states hence smoothing out learning and avoiding these oscillations or divergence during the gradient descent [15].

In constructing an environment that represents the wireless network, we use Python’s `gym` library which allows us to divide the observation space into discrete or continuous states, necessary for Q -learning to be able to learn. For this purpose, we build a power control algorithm using reinforcement learning. The states \mathcal{S} are discretizations of the environment observations which include the current received SINR, the received SINR after power control, and the power control command. Power control commands can increase or decrease the power as dictated by the codebook $\Gamma := \{-3, -1, 1, 3\}$ dB. We define a target SINR which the power control aspires to achieve. The instantaneous reward R is computed in terms of the difference in SINR after the power control command was implemented. The set of actions \mathcal{A} has the following elements:

- a_0 advances to the next value in the power control codebook,
- a_1 retracts to the previous value in Γ , and
- a_2 does nothing.

Further Use Cases: Other problems that can be solved with reinforcement learning are joint power control and interference coordination [9], link adaptation improvement, resource scheduling, and optimal predictive beam allocation.

VIII. PERFORMANCE MEASURES

Two groups of performance measures in the source code are observed and defined below. For the radio performance measures, the symbols refer to the model-based development in Section IV.

A. Radio Performance Measures

- 1) **Error vector:** Defined as the difference of the vectorized channel estimate from the true vectorized channel. Therefore, $\mathbf{e} := \text{vec}(\mathbf{H}) - \text{vec}(\hat{\mathbf{H}})$.

- 2) **Estimation mean squared error:** Defined as the square of the Euclidean norm divided by the number of elements in the channel matrix. Thus $\text{MSE} := \|\mathbf{e}\|^2 / (N_r N_t)$.
- 3) **Information bit rate (C):** This is the payload size (in bits) divided by the transmit time interval (in seconds) for units of bits/s. It is further related to the spectral efficiency SE as $C = B \cdot \text{SE} = \Delta f N_{\text{sc}} r \log_2 M$.
- 4) **Sum rate capacity:** This is a generalization of the information bit rate across multiple streams. For example, in SM, we write the sum rate as $C = \sum_{j=1}^{N_s} B_j \log_2(1 + \gamma_j)$.
- 5) **Bit error rate (BER):** Defined as the number of bits received incorrectly relative to the total number of bits transmitted across all antennas.
- 6) **Block error rate (BLER):** Defined at the receiver as the number of transmissions the CRC of which is incorrect divided by the total number of transmissions (Hence, $\text{BLER} := \mathbb{P}[\mathcal{P}(\mathbf{x}) \oplus \mathcal{P}(\hat{\mathbf{x}}) \neq 0]$, with $\mathcal{P}(\cdot)$ being the CRC polynomial generator function). Note that if this polynomial were set to all-ones, the BLER would become equal to $1 - (1 - \text{BER})^{L_{\text{codeword}}}$ since the bit errors are independent and identically distributed.

B. Machine Learning Performance Measures

These measures are meant for supervised learning only since the ground truth is known. Let us call the ground truth \mathbf{y} and the predicted value based on the machine learning prediction $\hat{\mathbf{y}}$.

- **Accuracy:** Defined as the complement of the mean classification error: $\frac{1}{M} \sum_{i=1}^M \mathbb{1}[[\mathbf{y}]_i \neq [\hat{\mathbf{y}}]_i]$. Note that accuracy can become meaningless if one category has rare occurrence since the classifier points to the majority class [16].
- **Precision and recall:** Used when the classification is imbalanced and the classes are not distributed equally or close enough. The reader is invited to look up their definition in other references (e.g., [7]).

While these measures are easier to explain in a binary classification, it is more difficult—though still relevant—for multi-class classification. There are other measures that can be used, such as the F1 score and the receiver operating characteristic area under the curve, which we invite the reader to look up.

For regression, the root MSE, MSE, and MAE quantities are all used as performance measures (besides being *de jure* loss functions). The *normalized* MSE (NMSE), defined as the MSE divided by the variance of the ground truth σ_y^2 , has gained popularity in recent publications despite being suitable for linear relationships. In addition, the coefficient of determination (R^2) can also be used,

though it is meaningful in linear regression. Otherwise for non-linear relations, imposing a high bias model (in our case a linear relationship) can cause this quantity to be negative. Definition of bias and the bias-variance trade-off can be found in several references (e.g., [16]). There are suitable measures for non-linear relationships such as the maximal information coefficient, which the reader is also invited to look up.

IX. USING THE CODE

Libraries: Deepwireless can be installed through pip from a terminal window (e.g., UNIX shell or Command Prompt) as follows:

```
pip3 install deepwireless
```

Python 3.13 needs to be installed on the machine that uses deepwireless. The more advanced user can download deepwireless and make changes from the GitHub location (Git needs to be installed on the same machine):

```
git clone https://github.com/farismismar/deepwireless
```

Scenarios: The source code implementing the various use cases in this primer can be downloaded from [1]. There are two source files (in addition to the libraries above): The first file `scenario_one.py` implements the parameters in Table II for a model-driven implementation of a wireless system. The reader should try and adjust these parameters to develop a basic understanding and become familiar with the code. The second file `scenario_two.py` implements all the other use cases in the data-driven implementation (i.e., supervised learning, unsupervised learning, autoencoders, and reinforcement learning). These two scenario files are found under the `test` folder with other auxiliary files (i.e., `autoencoder.py`, `DQNLearningAgent.py`, `QLearningAgent.py`, and `environment.py`) being reusable with minimal modifications.

Code Execution and Output: The code can be run either from a terminal window (e.g., `python3 <file>.py`), where `<file>.py` is a placeholder, or an integrated development environment (IDE). IDEs offer several advantages over terminal windows such as debugging, faster code development, and display of plots inline. The output of the run of the model-based part (i.e., `scenario_one.py`) is two dataframes `df_detailed_results` and `df_results`. These files contain the radio performance measures as defined in Section VIII.

The run of the data-driven part `scenario_two.py` has several outputs depending on the use case. The CNN learning part returns the received noisy and rotated symbols, the transmitted symbols, and the denoised data after equalization using the CNN. The LSTM learning part

TABLE II
SYSTEM PARAMETERS

Parameter	Description	Python
Random seed	This is the seed used by the pseudo-random number generator. Helps with reproducibility of results.	<code>seed = 42</code>
Number of transmit antennas (N_t)	The number of rows in the channel \mathbf{H} .	<code>N_t = 4</code>
Number of receive antennas (N_r)	The number of columns in the channel \mathbf{H} .	<code>N_r = 4</code>
Number of OFDM subcarriers per symbol (N_{sc})	These subcarriers determine the transmission bandwidth.	<code>N_sc = 64</code>
Total transmit power [W] (P_{total})	This is the transmit power across all antennas.	<code>transmit_power = 1</code>
OFDM subcarrier spacing [Hz] (Δf)	Determines the OFDM transmission bandwidth and the OFDM subcarrier spacing.	<code>Df = 15e3</code>
Center frequency [Hz] (f_c)	The center frequency of the transmit band. Used for the large-scale fading and the computation of the DFT.	<code>f_c = 1800e6</code>
Precoder (\mathbf{F})	This is the channel precoder (identity, SVD, SVD and waterfilling, and DFT beamforming).	<code>precoder = 'identity'</code>
Channel type	Specifies the channel model (CDL-A, CDL-C, CDL-E, Rayleigh, Ricean, and DeepMIMO [17]).	<code>channel_type = 'CDL-E'</code>
Path loss model	Selects a model for large scale fading.	<code>pathloss_model = 'FSPL'</code>
Payload mode	Random or defined by an 8-bit 32×32 bitmap file.	<code>payload_mode = 'random'</code>
Interference power [dBm] (σ_i^2)	This implements an additive Gaussian interference source at the receiver.	<code>interference_power_dBm = -105</code>
Interference probability ($p_{interference}$)	Probability of the interference occurring on a subcarrier.	<code>p_interference = 0.00</code>
Constellation (\mathcal{C})	This is the modulation scheme of the OFDM subcarriers.	<code>constellation = 'QAM'</code>
Constellation size (M)	Number of symbols in the constellation. Must be a power of two.	<code>M_constellation = 16</code>
Maximum number of transmissions	The number of full $N_t \times N_{sc}$ OFDM subcarriers to be transmitted (this can be converted to payload size in bits).	<code>max_transmission = 700</code>
CRC generator $\mathcal{P}(\mathbf{x})$	A string of bits that represent the CRC generator polynomial.	<code>crc_polynomial = 0b1100_0100</code>
Channel compression ratio (κ)	The ratio at which the channel \mathbf{H} is compressed at the transmitter before it is sent to be reconstructed at the receiver (set to zero for no compression).	<code>channel_compression_ratio = 0.00</code>
Number of pilot symbols (n_{pilot})	Length of pilots sequence required for channel estimation (at least equal to N_t).	<code>n_pilot = None</code>
Transmit SNR [dB] (ρ)	The transmitted signal SNR.	<code>transmit_SNR_dB = [-10, -5, 0, 5, 10, 15, 20, 25, 30]</code>
Channel estimation algorithm for MIMO channel	This specifies the algorithm used to estimate the transmit channel (i.e., perfect, LMMSE, and LS).	<code>MIMO_estimation = 'perfect'</code>
Channel equalization algorithm	Specifies the algorithm used to equalize the estimated channel (i.e., MMSE and ZF).	<code>MIMO_equalization = 'MMSE'</code>
Symbol detection algorithm	Specifies the algorithm used to detect the OFDM symbols transmitted (i.e., max likelihood, k-means, ensemble, and DNN).	<code>symbol_detection = 'ML'</code>
Independent variable	A quantity from the radio performance measures in Section VIII.	<code>x_label = 'EbN0_dB'</code>
Dependent variable	A quantity from the radio performance measures in Section VIII.	<code>y_label = 'BER'</code>

returns the predicted time series along with the model score. The reinforcement learning part returns a group of variables: `Q_values`, `losses`, `optimal_episode`, `optimal_reward`, `optimal_environment_progress`, and `optimal_action_progress`. The last two variables are actually based on the actions and states which are dictated by the environment and the optimization objective. We also show output plots in Figs. 5-13 below.

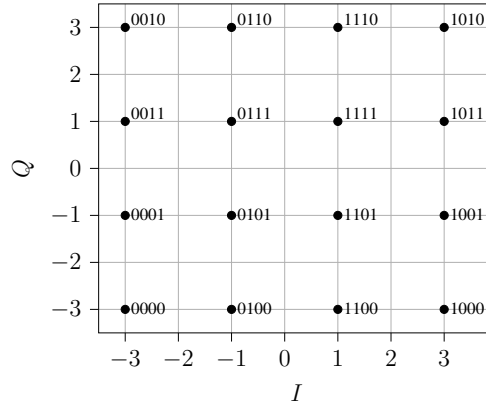
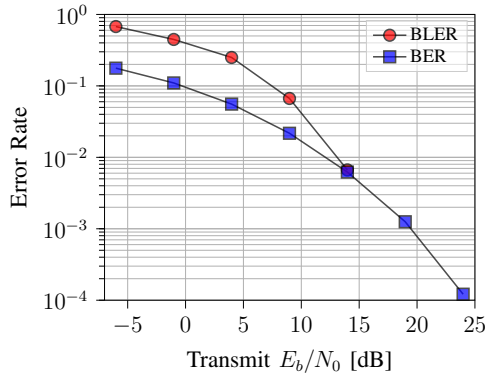
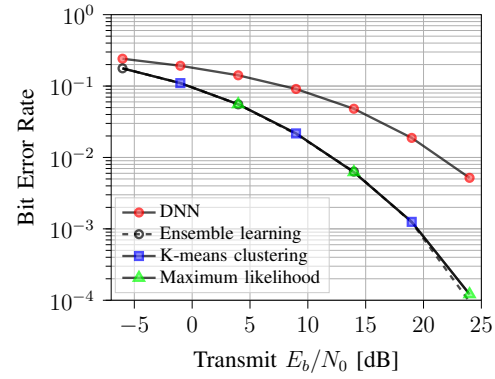


Fig. 5. 16-QAM constellation with Gray code which for any two adjacent symbols only a change of one bit is permissible.

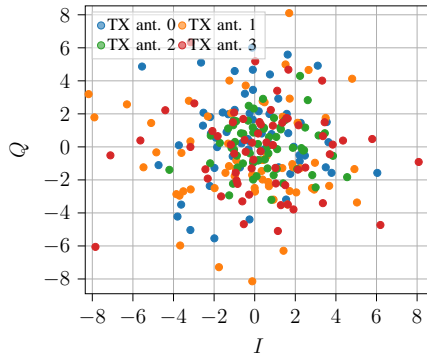


(a) BLER and BER vs E_b/N_0

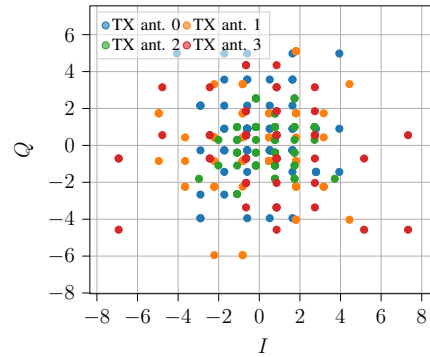


(b) BER vs E_b/N_0 with machine learning

Fig. 6. Bit and block error rate performance curve (left) and bit error rate performance curve for three different algorithms (right). The curves are for a MIMO system using 16-QAM and the parameters as shown in Table II.



(a) Without quantization



(b) With quantization ($b = 3$)

Fig. 7. Received signal constellation plot without (left) and with quantization at $b = 3$ (right).

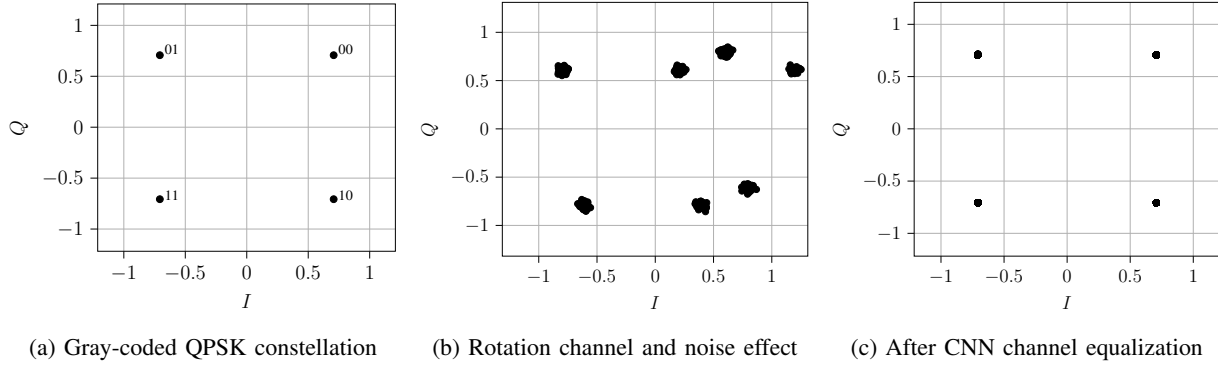


Fig. 8. CNNs equalizing a rotation channel with the presence of shot noise (using QPSK constellation). In this case, $\rho = 30$ dB and $\theta = \pi/24$.

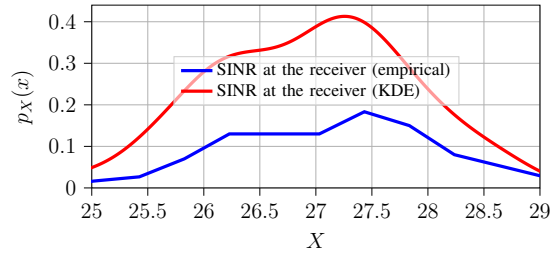


Fig. 9. The empirical and KDE-based PDF of the received SINR at $\rho = 30$ dB.

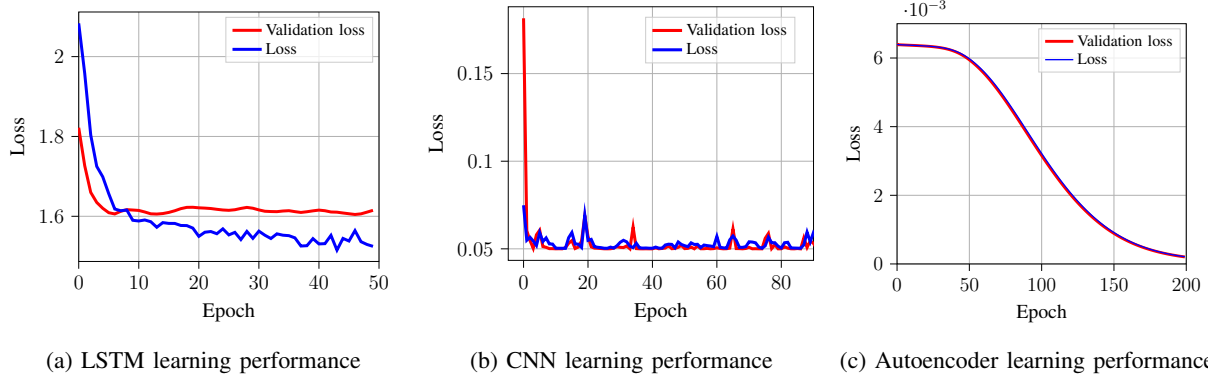


Fig. 10. Deep learning performance: LSTM learning performance in proactive beam prediction (left), CNN learning performance in rotation channel equalization, and autoencoders learning performance for channel compression (right).

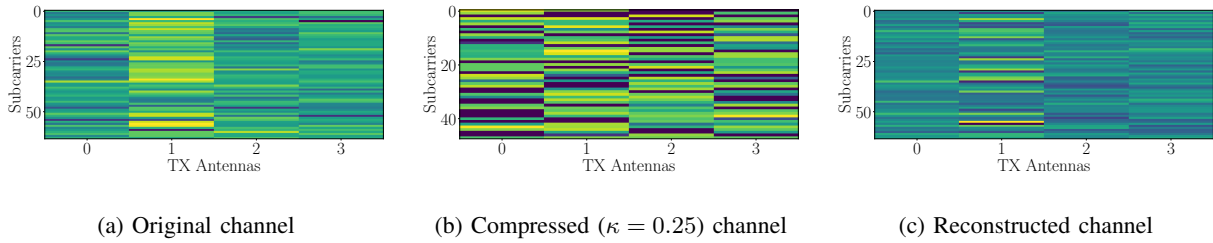


Fig. 11. Channel compression of a CDL-E channel (4×4 MIMO and 64 OFDM subcarriers) and its reconstruction using deep autoencoders.

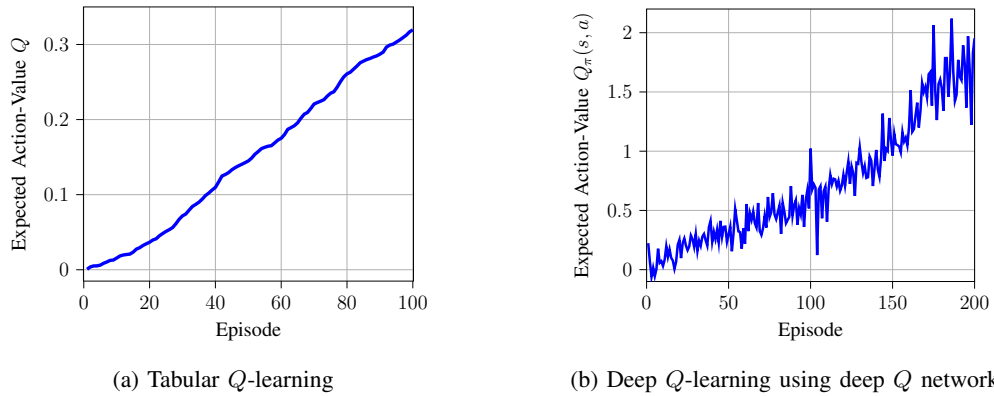


Fig. 12. Q -learning using tabular (left) and deep learning (right). The experience as measured by the value of $Q_\pi(s, a)$ goes up with more training episodes.

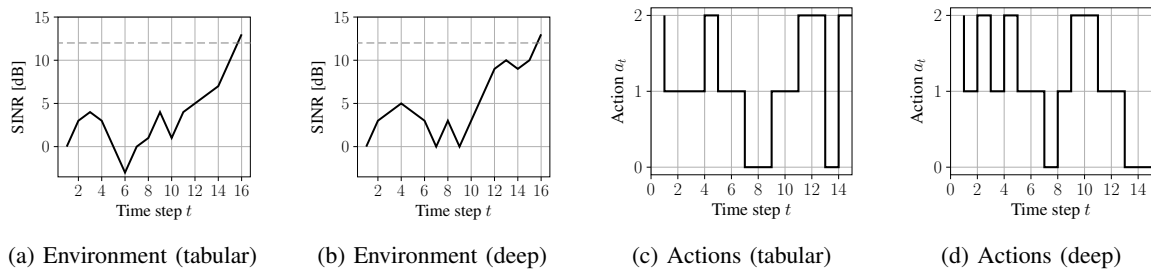


Fig. 13. The result of the interaction between the environment and the tabular and deep Q -learning algorithms.

X. FURTHER TOPICS

Congratulations on making it this far into this primer! We hope that it has kindled in you the desire to walk this path in your learning or research. For this purpose, we leave a few more topics for you to consider as you probe further.

- Generative Adversarial Networks (GANs): GANs can also be applied in the wireless space. Pilot-free channel estimation out of band is a good example. Using measurements of an existing band (e.g., a heatmap) or the CSI, and a few measurements of an out of band spectrum, can a GAN generate the entire heatmap for the measurements (or the CSI) of this out of band carrier?
- Large Language Models (LLMs): While mostly text-based, LLMs have demonstrated an ability to provide insights that can be used towards intelligent automation with human supervision. For example, generation of corrective actions (e.g., configuration scripts) for the network operation center to use as a solution for a network fault event.

These two topics fall into what is collectively known today “Generative AI” (as opposed to discriminative AI). In the space of wireless communications, here are a few more topics to consider as next steps:

- Multiple OFDM symbols: Currently a single OFDM symbol is used in the simulator. Realistic systems have more OFDM symbols per time slot. For example, both 4G LTE and NR have 7 OFDM symbols per timeslot (0.5 ms).
- Forward error correction can further improve the system performance due to coding gain. LDPC outperforms Turbo codes at high code rates, while Turbo codes outperform LDPC when the code rate is low.
- Multiple concurrent users to enable SDMA or multi-user MIMO (potentially with mobility and Doppler effect addressed).
- Link adaptation: Optimize coding schemes and modulation to improve the BLER curve performance beyond current standards.

XI. CONCLUSION

In this primer, we summarized the various concepts required to build a wireless communication prototype that supports a single OFDM symbol MIMO system. We showed how the prototype can be implemented in Python using the deepwireless library and showed a few use cases of machine learning (supervised, self-supervised, and unsupervised) and reinforcement learning across few layers in the air interface protocol stack. As this is our final issue, we hope that both clarity and flow have made reading this primer beneficial to the reader. Feedback is always welcome.

REFERENCES

- [1] F. B. Mismar, "Source Code," May 2025. [Online]. Available: <https://github.com/farismismar/deepwireless>
- [2] 3GPP, "5G; Study on channel model for frequencies from 0.5 to 100 GHz," 3rd Generation Partnership Project, TR 38.901, Jun. 2018.
- [3] J. G. Proakis and M. Salehi, *Digital Communications*, 5th ed. McGraw-Hill, 2008.
- [4] A. F. Molisch, *Wireless Communications*, 2nd ed. Wiley Publishing, 2011.
- [5] F. B. Mismar and J. Hoydis, "Unsupervised Learning in Next-Generation Networks: Real-Time Performance Self-Diagnosis," *IEEE Communications Letters*, vol. 25, no. 10, pp. 3330–3334, 2021.
- [6] S. Liu, R. De Lacerda, and J. Fiorina, "WKNN Indoor Wi-Fi Localization Method using k-means Clustering Based Radio Mapping," in *Proc. IEEE 93rd Vehicular Technology Conference*, Apr. 2021, pp. 1–5.
- [7] I. J. Goodfellow, Y. Bengio, and A. Courville, *Deep Learning*. Cambridge, MA, USA: MIT Press, 2016. [Online]. Available: <http://www.deeplearningbook.org>
- [8] F. B. Mismar and A. O. Kaya, "Adaptive Compression of Massive MIMO Channel State Information With Deep Learning," *IEEE Networking Letters*, vol. 4, no. 6, 2024.
- [9] F. B. Mismar, B. L. Evans, and A. Alkhateeb, "Deep Reinforcement Learning for 5G Networks: Joint Beamforming, Power Control, and Interference Coordination," *IEEE Transactions on Communications*, vol. 68, no. 3, pp. 1581–1592, 2020.
- [10] F. B. Mismar and B. L. Evans, "Partially Blind Handovers for mmWave New Radio Aided by Sub-6 GHz LTE Signaling," in *Proc. IEEE International Conference on Communications Workshop*, May 2018, pp. 1–5.
- [11] F. B. Mismar, A. AlAmmouri, A. Alkhateeb, J. G. Andrews, and B. L. Evans, "Deep Learning Predictive Band Switching in Wireless Networks," *IEEE Trans. on Wirel. Commun.*, vol. 20, no. 1, pp. 96–109, 2021.
- [12] F. B. Mismar and B. L. Evans, "Deep Learning in Downlink Coordinated Multipoint in New Radio Heterogeneous Networks," *IEEE Wireless Communications Letters*, vol. 8, no. 4, pp. 1040–1043, 2019.
- [13] F. B. Mismar, A. Gündoğan, A. O. Kaya, and O. Chistyakov, "Deep Learning for Multi-User Proactive Beam Handoff: A 6G Application," *IEEE Access*, vol. 11, pp. 46 271–46 282, 2023.
- [14] R. S. Sutton and A. G. Barto, *Reinforcement Learning: An Introduction*. Cambridge, MA, USA: MIT press, Oct. 2018.
- [15] V. Mnih, K. Kavukcuoglu, D. Silver, A. Graves, I. Antonoglou, D. Wierstra, and M. Riedmiller, "Playing Atari with Deep Reinforcement Learning," 2013. [Online]. Available: <https://arxiv.org/abs/1312.5602>
- [16] C. M. Bishop, *Pattern Recognition and Machine Learning (Information Science and Statistics)*. Berlin, Heidelberg: Springer-Verlag, 2006. [Online]. Available: <https://www.microsoft.com/en-us/research/uploads/prod/2006/01/Bishop-Pattern-Recognition-and-Machine-Learning-2006.pdf>
- [17] A. Alkhateeb, "DeepMIMO: A Generic Deep Learning Dataset for Millimeter Wave and Massive MIMO Applications," in *Proc. of Information Theory and Applications Workshop*, San Diego, CA, Feb. 2019, pp. 1–8.